

# Exploring the Variable Hapticity of the Arylamide Ligand: Access to $\sigma$ -Amidophenyl and $\pi$ -Cyclohexadienylimine Structures

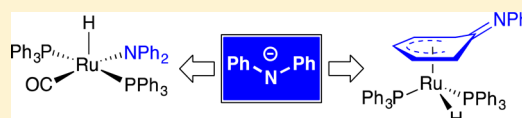
Benjamin J. Ireland,<sup>†</sup> Robert McDonald,<sup>‡</sup> and Deryn E. Fogg<sup>\*,†</sup>

<sup>†</sup>Center for Catalysis Research & Innovation and Department of Chemistry, University of Ottawa, Ottawa, Ontario, Canada K1N 6N5

<sup>‡</sup>X-ray Crystallography Laboratory, Chemistry Department, University of Alberta, Edmonton, Alberta, Canada T6G 2G2

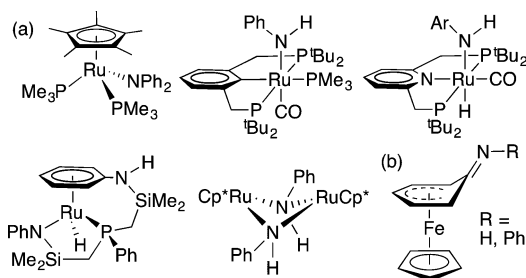
## Supporting Information

**ABSTRACT:** A study of the preference for  $\sigma$  vs  $\pi$  coordination of the arylamido ligand to a late transition metal shows that  $\text{LiNPh}_2$  reacts with  $\text{RuHCl}(\text{PPh}_3)_3$  (**1**) to yield the bent-seat piano-stool complex  $\text{RuH}[(\eta^5\text{-C}_6\text{H}_5)\text{NPh}](\text{PPh}_3)_2$  (**2a**) but with  $\text{RuHCl}(\text{CO})(\text{PPh}_3)_3$  (**3**) to yield the  $\sigma$ -amide  $\text{RuH}(\eta^1\text{-NPh}_2)(\text{CO})(\text{PPh}_3)_2$  (**4**). The stability of the  $\sigma$ -bound  $\text{NPh}_2$  ligand in **4** reflects the  $\pi$  acidity of the CO ligand, which inhibits  $\text{PPh}_3$  loss. Carbonylation of **2a** at 50 °C affords  $\text{Ru}(\text{CO})_3(\text{PPh}_3)_2$  (**8**) and  $\text{HNPh}_2$ , suggesting sequential  $\pi \rightarrow \sigma$  isomerization and reductive elimination. The phenoxide ligand behaves similarly:  $\text{RuH}(\eta^5\text{-C}_6\text{H}_5\text{O})(\text{PPh}_3)_2$  (**2b**) is formed from **1** but  $\text{RuH}(\eta^1\text{-OPh})(\text{CO})(\text{PPh}_3)_3$  (**5**) is formed from **3**, and carbonylation of **2b** gives **8** and phenol, although more forcing conditions are required (90 °C). The crystal structure of **2a** is reported.



Examples of amido complexes of the late transition metals have expanded greatly in recent years, driven largely by interest in their catalytic properties.<sup>1–3</sup> Arylamido ligands are of particular interest for their potential steric and electronic tunability. In the dominant anido derivatives, the anionic nitrogen is typically monodentate or bridging (Chart 1a),<sup>1–3</sup> but the  $\eta^5$ -cyclohexadienylimine structure (Chart 1b) is also known.<sup>4,5</sup> Analogous bent-seat piano-stool complexes are well documented in Ru–aryloxide chemistry.<sup>6–11</sup>

**Chart 1.** (a) Selected  $\text{Ru}(\sigma\text{-NRAr})$  Derivatives<sup>15–19</sup> and (b)  $\eta^5$ -Cyclohexadienylimine Complexes of Iron<sup>4,5</sup>

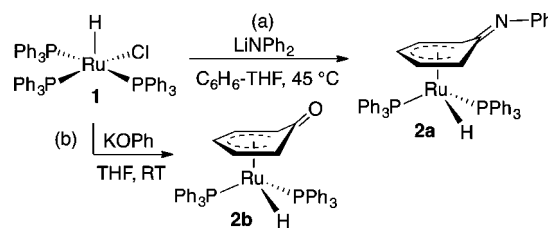


The potential for reversible isomerization between such  $\sigma$ - and  $\pi$ -bound structures is of interest in catalysis, as it may affect the lifetime and productivity of coordinatively unsaturated  $\sigma$ -NRAr complexes. We earlier suggested that  $\text{Ru}(\pi\text{-OAr})$  structures may be expected for monodentate aryloxides wherever the ancillary ligands are sufficiently labile to give access to the required three coordination sites.<sup>10</sup> Subsequent work demonstrated that binaphtholate complexes of ruthenium can adapt between the extremes of  $\eta^1:\eta^1$  and  $\eta^3:\eta^3$  binding, depending on the number of other ligands present.<sup>12–14</sup> Here

we report a study of the  $\text{RuHX}'(\text{PPh}_3)_n$  system, a well-developed model that enables examination of these effects without the difficulties associated with identification of metal complexes formed during catalysis. We provide evidence that the arylamide ligand can likewise adapt its hapticity and that it may do so even more readily than phenoxide. For either ligand class, however, incorporation of a single  $\pi$ -acid carbonyl ligand proves sufficient to bias selectivity toward the  $\sigma$ -EAr<sub>n</sub> coordination mode (E = O, N).

Addition of  $\text{Li}[\text{NPh}_2]$  as a solution in THF to a purple suspension of  $\text{RuHCl}(\text{PPh}_3)_3$  (**1**) in benzene caused a color change to orange within 15 min at 45 °C. Formation of  $\text{RuH}[(\eta^5\text{-C}_6\text{H}_5)\text{NPh}](\text{PPh}_3)_2$  (**2a**) (Scheme 1a) was complete within 1 h, as judged by  $^31\text{P}\{^1\text{H}\}$  NMR analysis. The sole species observed in the crude reaction mixture were free  $\text{PPh}_3$  and **2a** (molar ratio 1/1). Pale orange **2a** was isolated in 73% yield after workup. X-ray-quality crystals deposited from toluene–hexanes at –30 °C.

**Scheme 1.** Piano-Stool Products Formed by Reaction of  $\text{RuHCl}(\text{PPh}_3)_3$  with Diphenylamide or Phenoxide<sup>10</sup>



Received: June 7, 2013

Crystallographic analysis of **2a** (Figure 1) reveals that the amide ligand is bound to the metal via an  $\eta^5$ -cyclohexadienyl

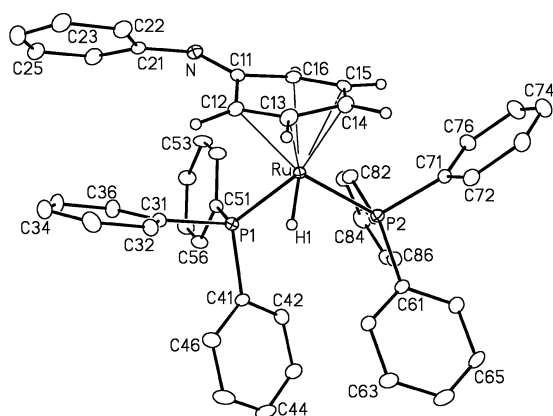


**Figure 1.** Perspective view of **2a**. Non-hydrogen atoms are represented by Gaussian ellipsoids at the 20% probability level. The hydride ligand is shown with an arbitrarily small thermal ellipsoid. Key metrics: C21–N, 1.406(6) Å; C11–N, 1.313(6) Å; C21–N–C11, 120.9(4)°.

ring. Loss of aromaticity is evident from the nonplanar structure of the ring, C11 being bent by 24° out of the plane. Partial imine character is suggested by the short N–C11 bond distance of 1.313(6) Å; cf. a value of 1.406(6) Å for the unperturbed NPh moiety and N=C bond lengths of ca. 1.26–1.27 Å for related aniline-derived ketimines.<sup>20–22</sup> The 120.9(4)° angle for the C11–N–C21 bond is consistent with formulation as an imine.

NMR analysis of **2a** confirms the distorted piano-stool structure. Diagnostic <sup>1</sup>H NMR markers for the  $\eta^5$ -bound ring are depicted in Figure 2. Five NC<sub>6</sub>H<sub>5</sub> signals are shifted

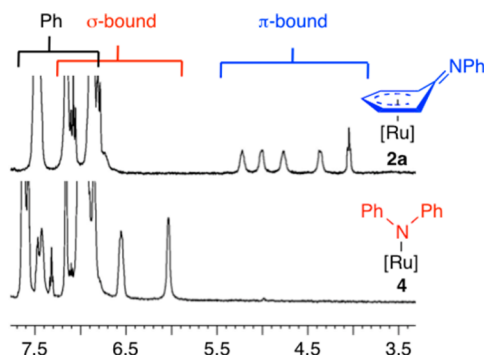
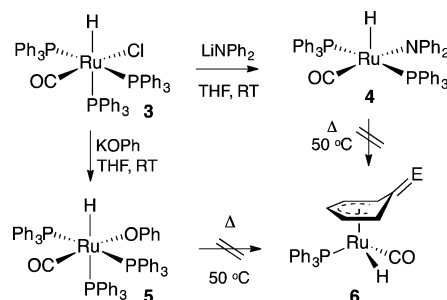


**Figure 2.** Diagnostic <sup>1</sup>H NMR locations (C<sub>6</sub>D<sub>6</sub> solvent) for the  $\sigma$ - and  $\pi$ -bound N(C<sub>6</sub>H<sub>5</sub>)<sub>2</sub> ligand in **2a** and **4**.

dramatically upfield from the aromatic region: they appear at ca. 4.0–5.3 ppm vs the region of 6.6–7.7 ppm occupied by the remaining phenyl protons. A hydride triplet appears at –11.94 (t, <sup>2</sup>J<sub>PH</sub> = 33 Hz). The quaternary imine carbon appears at 152.5 ppm; cf. a value of 175.6 ppm reported for Cy=NPh in CDCl<sub>3</sub>.<sup>23</sup> Similar structural and <sup>1</sup>H NMR data were reported for the  $\eta^5$ -C<sub>6</sub>H<sub>5</sub>O moiety in the known **2b** (Scheme 1b).<sup>6,7</sup>

To assess the impact of a  $\pi$ -acid ligand on the preferred coordination mode of the anionic donor, we explored the corresponding reaction of RuHCl(CO)(PPh<sub>3</sub>)<sub>3</sub> (**3**) with LiNPh<sub>2</sub>. A color change from white to red occurred over 15 min at 23 °C in THF, with full conversion to RuH( $\sigma$ -NPh<sub>2</sub>)(CO)(PPh<sub>3</sub>)<sub>2</sub> **4** (Scheme 2) after 1 h. <sup>31</sup>P{<sup>1</sup>H} NMR

### Scheme 2. $\sigma$ -Arylamide and $\sigma$ -Aryloxide Complexes Accessible from RuHCl(CO)(PPh<sub>3</sub>)<sub>3</sub>

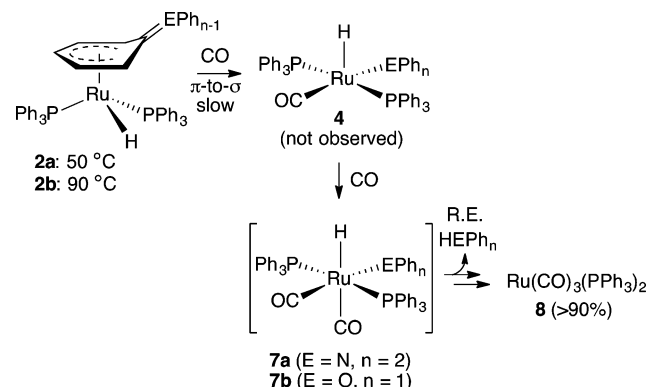


analysis of crude **4** revealed a singlet at 41.7 ppm, accompanying that for equimolar free PPh<sub>3</sub>. Additional Ru species present in minor amounts include known<sup>24</sup> RuH<sub>2</sub>(CO)(PPh<sub>3</sub>)<sub>3</sub> and unidentified hydride coproducts that give rise to signals between –3 and –8.5 ppm. Clean **4** was isolated in 76% yield after washing with hexanes.

The hydride signal for **4**, a triplet at –17.19 ppm (<sup>2</sup>J<sub>PH</sub> = 22 Hz), is ca. 5 ppm upfield of that for **2a**. These data imply a square-pyramidal structure with an apical hydride and two mutually trans phosphine ligands.  $\sigma$  coordination of the diphenylamide ligand is confirmed by the downfield location of all phenyl signals in the <sup>1</sup>H NMR spectrum (6.0–7.7 ppm; Figure 2).

The  $\sigma$ -bound amide ligand in **4** does not convert into the  $\pi$  structure **6** over 24 h at 50 °C (C<sub>6</sub>D<sub>6</sub>; <3% loss vs internal standard). We attribute this stability to the presence of the  $\pi$ -acid CO ligand, which inhibits phosphine loss. Treating piano-stool complex **2a** with CO, however, triggers release of HNPh<sub>2</sub> and formation of Ru(CO)<sub>3</sub>(PPh<sub>3</sub>)<sub>2</sub> (**8**),<sup>25</sup> most plausibly via reductive elimination of HNPh<sub>2</sub> from RuH( $\sigma$ -NPh<sub>2</sub>)(CO)<sub>2</sub>(PPh<sub>3</sub>)<sub>2</sub> (**7a**) (Scheme 3). Formation of **8** reaches 92%

### Scheme 3. Proposed Pathway for Carbonylation of **2a,b** To Form HEPPh<sub>n</sub> and Ru(CO)<sub>3</sub>(PPh<sub>3</sub>)<sub>2</sub> (**8**)



in 2 h at 50 °C. The potential intermediacy of **4** was verified by exposing **4** to CO: this effected complete conversion into **8** and HNPh<sub>2</sub> within 2 h at 50 °C. Room-temperature experiments indicated that the reductive elimination step was considerably faster for **4** than for **2a**. For **4**, evolution of HNPh<sub>2</sub> reached 90% within 20 min vs 65% for **2a** at 24 h. Initial  $\pi \rightarrow \sigma$  isomerization of phenylamide thus appears to be the principal barrier to carbonylation of **2a**. (The higher proportion of HNPh<sub>2</sub> than **8** (Table S1 in the Supporting Information) also indicates that reductive elimination occurs prior to formation of **8**.) Attempts

to independently prepare **7a** by treating  $\text{RuHCl}(\text{CO})_2(\text{PPh}_3)_2$  with  $\text{LiNPh}_2$  yielded ca. 1/1 **4** and **8**: while the observed CO disproportionation is unexpected, this finding confirms the instability of **7a** toward reductive elimination.

The generality of this arylamide behavior is demonstrated by the accessibility of a  $\sigma$ -aryloxo complex related to **4** via addition of  $\text{KOPh}$  to **3**. The reaction was complete within 2 h at room temperature in THF, and clean  $\text{RuH}(\sigma\text{-OPh})(\text{CO})\text{-}(\text{PPh}_3)_3$  (**5**) was obtained as a white powder in 91% yield (Scheme 2). Retention of all three phosphine ligands in **5**—a function of the reduced bulk of the OPh ligand, relative to the  $\text{NPh}_2$  ligand in **4**—is indicated by the multiplicity and location of the hydride signal, which appears as a doublet of triplets at  $-6.63$  ppm ( $^2J_{\text{HP}} = 112$  and 24 Hz). Other spectroscopic data are consistent with the proposed structure. Thus, the room-temperature  $^{31}\text{P}\{^1\text{H}\}$  NMR spectrum revealed two broad singlets at 38.1 and 16.3 ppm (ratio 2:1;  $\text{C}_6\text{D}_6$ ), which resolve into an  $\text{A}_2\text{B}$  pattern ( $^2J_{\text{PP}} = 17$  Hz) at 263 K in  $\text{C}_7\text{D}_8$ .

As with the arylamide derivatives, aryloxo **5** resisted  $\sigma \rightarrow \pi$  isomerization at 50 °C, but thermolysis of piano-stool complex **2b** at 90 °C under CO liberated **8** and phenol (Scheme 3; 93% after 6 h). No reaction was observed over 24 h at 50 °C, suggesting a higher barrier to  $\pi \rightarrow \sigma$  isomerization of phenoxide than for diphenylamide.

The foregoing demonstrates that monodentate arylamide and aryloxo ligands exhibit qualitatively similar tendencies in terms of the parameters that favor  $\sigma$  binding via the heteroatom vs  $\pi$  coordination via a dearomatized ring. For either ligand class, piano-stool structures are favored where three binding sites are available. When the lability of the  $\text{PPh}_3$  ligands is restricted—even by introduction of a single CO ligand— $\sigma$ -arylamide or -aryloxo derivatives are formed. In the presence of additional ligands, however, the piano-stool complexes can slip to lower-hapticity structures. Exposure to CO is shown to induce  $\pi \rightarrow \sigma$  interconversion and reductive elimination of diphenylamine or phenol. Of note is the lower barrier of this transformation for the amido complex, which may indicate that the arylamide ligand adjusts its hapticity to accommodate incoming ligands more readily than does aryloxo. This potential advantage may be offset, for hydride derivatives, by relatively facile reductive elimination. Whether nonhydride derivatives also readily eject the arylamide ligand is presently under study.

## ■ ASSOCIATED CONTENT

### Supporting Information

Text, figures, tables, and a CIF files giving experimental and crystallographic details. This material is available free of charge via the Internet at <http://pubs.acs.org>.

## ■ AUTHOR INFORMATION

### Corresponding Author

\*E-mail for D.E.F.: [dfogg@uottawa.ca](mailto:dfogg@uottawa.ca).

### Notes

The authors declare no competing financial interest.

## ■ ACKNOWLEDGMENTS

This work was funded by the NSERC of Canada. The NSERC is thanked for a CGS-D award to B.J.I.

## ■ REFERENCES

- (1) Lappert, M.; Protchenko, A.; Power, P.; Seeber, A. *Metal Amide Chemistry*; Wiley: Chichester, U.K., 2009.
- (2) Fulton, J. R.; Holland, A. W.; Fox, D. J.; Bergman, R. G. *Acc. Chem. Res.* **2002**, *35*, 44–56.
- (3) Ikariya, T. *Bull. Chem. Soc. Jpn.* **2011**, *84*, 1–16.
- (4) Helling, J. F.; Hendrickson, W. A. *J. Organomet. Chem.* **1977**, *141*, 99–105.
- (5) Helling, J. F.; Hendrickson, W. A. *J. Organomet. Chem.* **1979**, *168*, 87–95.
- (6) Cole-Hamilton, D. J.; Young, R. J.; Wilkinson, G. *J. Chem. Soc., Dalton Trans.* **1976**, 1995–2001.
- (7) Yamamoto, T.; Miyashita, S.; Naito, Y.; Komiya, S.; Ito, T.; Yamamoto, A. *Organometallics* **1982**, *1*, 808–812.
- (8) Chaudret, B.; He, X.; Huang, Y. *J. Chem. Soc., Chem. Commun.* **1989**, 1844–1846.
- (9) Christ, M. L.; Sabo-Etienne, S.; Chung, G.; Chaudret, B. *Inorg. Chem.* **1994**, *33*, 5316–19.
- (10) Snelgrove, J. L.; Conrad, J. C.; Yap, G. P. A.; Fogg, D. E. *Inorg. Chim. Acta* **2003**, *345*, 268–278.
- (11) Abdur-Rashid, K.; Fedorkiw, T.; Lough, A. J.; Morris, R. H. *Organometallics* **2004**, *23*, 86–94.
- (12) Blacquiere, J. M.; Higman, C. S.; McDonald, R.; Fogg, D. E. *J. Am. Chem. Soc.* **2011**, *133*, 14054–14062.
- (13) Blacquiere, J. M.; McDonald, R.; Fogg, D. E. *Angew. Chem., Int. Ed.* **2010**, *49*, 3807–3810.
- (14) Panichakul, D.; Su, Y.; Li, Y.; Deng, W.; Zhao, J.; Li, X. *Organometallics* **2008**, *27*, 6390–6392.
- (15) Bryndza, H. E.; Fong, L. K.; Paciello, R. A.; Tam, W.; Bercaw, J. E. *J. Am. Chem. Soc.* **1987**, *109*, 1444–1456.
- (16) Zhang, J. B.; Gunnoe, T. B.; Boyle, P. D. *Organometallics* **2004**, *23*, 3094–3097.
- (17) Khaskin, E.; Iron, M. A.; Shimon, L. J. W.; Zhang, J.; Milstein, D. *J. Am. Chem. Soc.* **2010**, *132*, 8542–8543.
- (18) Fryzuk, M. D.; Petrella, M. J.; Coffin, R. C.; Patrick, B. O. *C. R. Chim.* **2002**, *5*, 451–460.
- (19) Blake, R. E., Jr.; Heyn, R. H.; Tilley, T. D. *Polyhedron* **1992**, *11*, 709–710.
- (20) Keim, W.; Killat, S.; Nobile, C. F.; Suranna, G. P.; Englert, U.; Wang, R.; Mecking, S.; Schröder, D. L. *J. Organomet. Chem.* **2002**, *662*, 150–171.
- (21) Schleis, T.; Heinemann, J.; Spaniol, T. P.; Mülhaupt, R.; Okuda, J. *Inorg. Chem. Commun.* **1998**, *1*, 431–434.
- (22) Markowicz, S. W.; Figlus, M.; Lejkowski, M.; Karolak-Wojciechowska, J.; Dzierżawska-Majewska, A.; Verpoort, F. *Tetrahedron: Asymmetry* **2006**, *17*, 434–448.
- (23) Barluenga, J.; Jiménez-Aquino, A.; Aznar, F.; Valdés, C. *J. Am. Chem. Soc.* **2009**, *131*, 4031–4041.
- (24) Hallman, P. S.; McGarvey, B. R.; Wilkinson, G. *J. Chem. Soc. A* **1968**, 3143–50.
- (25) Dell'Amico, D. B.; Calderazzo, F.; Labella, L.; Marchetti, F. *J. Organomet. Chem.* **2000**, *596*, 144–151.